

## Fermi-LAT Detection of a GeV Afterglow from a Compact Stellar Merger

HAI-MING ZHANG,<sup>1,2</sup> YI-YUN HUANG,<sup>1,2</sup> JIAN-HE ZHENG,<sup>1,2</sup> RUO-YU LIU,<sup>1,2</sup> AND XIANG-YU WANG<sup>1,2</sup>

<sup>1</sup>*School of Astronomy and Space Science, Nanjing University, Nanjing 210023, China; xywang@nju.edu.cn*

<sup>2</sup>*Key laboratory of Modern Astronomy and Astrophysics (Nanjing University), Ministry of Education, Nanjing 210023, China*

(Received 2022 May 22; Revised 2022 June 16; Accepted 2022 June 21)

### ABSTRACT

It is usually thought that long-duration gamma-ray bursts (GRBs) are associated with massive star core collapse, whereas short-duration GRBs are associated with mergers of compact stellar binaries. The discovery of a kilonova associated with a nearby (350 Mpc) long-duration GRB—GRB 211211A, however, indicates that the progenitor of this long-duration GRB is a compact object merger. Here we report the Fermi-LAT detection of gamma-ray ( $> 100$  MeV) afterglow emission from GRB 211211A, which lasts  $\sim 20,000$  s after the burst, the longest event for conventional short-duration GRBs ever detected. We suggest that this gamma-ray emission results from afterglow synchrotron emission. The soft spectrum of GeV emission may arise from a limited maximum synchrotron energy of only a few hundreds of MeV at  $\sim 20,000$  s. The unusually long duration of the GeV emission could be due to the proximity of this GRB and the long deceleration time of the GRB jet that is expanding in a low-density circumburst medium, consistent with the compact stellar merger scenario.

*Keywords:* Gamma-ray bursts — Magnetars

### 1. INTRODUCTION

Gamma-ray bursts (GRBs) are usually divided into two populations (Norris et al. 1984; Kouveliotou et al. 1993): long GRBs that originate from the core collapse of massive stars (Galama et al. 1998) and short GRBs formed in the merger of two compact objects (Abbott et al. 2017). While it is common to divide the two populations at a duration of 2 s for the prompt keV/MeV emission, classification based on duration only does not always correctly point to the progenitor. Growing observations (Ahumada et al. 2021; Gal-Yam et al. 2006; Gehrels et al. 2006; Zhang et al. 2021) have shown that multiple criteria (such as supernova/kilonova associations and host galaxy properties) rather than burst duration only are needed to classify GRBs physically.

GRB 211211A triggered the Burst Alert Telescope (BAT; Barthelmy et al. (2005)) on board the Neil Gehrels Swift Observatory at 13:09:59 UT (D’Ai et al. 2021), the Gamma-ray Burst Monitor (GBM; Meegan et al. (2009)) on board the Fermi Gamma-Ray Space Telescope at 13:09:59.651 UT (Mangan et al. 2021) and High energy X-ray Telescope on board Insight-HXMT (Xiao et al. 2022) at 13:09:59 UT on 2021 December 11. The burst is characterized by a spiky main emission phase lasting  $\sim 13$  s, and a longer, weaker extended emission phase lasting  $\sim 55$  s

(Yang et al. 2022). The prompt emission is suggested to be produced by the fast-cooling synchrotron emission (Gompertz et al. 2022). The discovery of a kilonova associated with this GRB indicates clearly that the progenitor is a compact object merger (Rastinejad et al. 2022). The event fluence (10-1000 keV) of the prompt emission is  $(5.4 \pm 0.01) \times 10^{-4}$  erg cm<sup>-2</sup>, making this GRB an exceptionally bright event. The host galaxy redshift of GRB 211211A is  $z = 0.0763 \pm 0.0002$  (corresponding to a distance of  $\approx 350$  Mpc; Rastinejad et al. (2022)). At 350 Mpc, GRB 211211A is one of the closest GRBs, a bit further than GRB 170817A, which is associated with the gravitational wave (GW)-detected binary neutron star (BNS) merger GW170817. For GRB 170817A, no GeV afterglow was detected by the Large Area Telescope (LAT) on timescales of minutes, hours, or days after the LIGO/Virgo detection (Ajello et al. 2018).

As the angle from the Fermi-LAT boresight at the GBM trigger time of GRB 211211A is 106.5 degrees (Mangan et al. 2021), LAT cannot place constraints on the existence of high-energy ( $E > 100$  MeV) emission associated with the prompt GRB emission. We focus instead on constraining high-energy emission on the longer timescale. We analyze the late-time Fermi-LAT data when the GRB enters the field-of-view (FOV) of Fermi-

LAT. We detect a transient source with a significance of  $TS_{\max} \simeq 51$ , corresponding to a detection significance over  $6\sigma$ . The result of the data analysis is shown in Section 2 and the interpretation of the origin of this GeV afterglow is given in Section 3. In Section 4, we give a brief summary.

## 2. FERMI-LAT DATA ANALYSIS

At 13:09:59 UT (denoted as  $T_0$ ), the Swift/BAT triggered and located GRB 211211A (D’Ai et al. 2021). The Fermi-LAT extended type data for the GRB 211211A was taken from the Fermi Science Support Center<sup>1</sup> from  $T_0 - 10$  days to  $T_0 + 10$  days. Only the data within a  $14^\circ \times 14^\circ$  region of interest (ROI) centered on the position of GRB 211211A are considered for the analysis (initially centred on Swift/X-ray Telescope (XRT) position). We select the observation time of GRB 211211A by LAT only when the angle from the Fermi-LAT bore-sight is less than  $100^\circ$ . The first observation starts at 395 s after Swift/BAT trigger, so we use the Source-class event selection, which has more stringent background rejection cuts than Transient-class events and is better suited for analyses of long time intervals and dimmer sources. We also select the events with energies between 100 MeV and 10 GeV, with a maximum zenith angle of  $100^\circ$  to reduce the contamination from the  $\gamma$ -ray Earth limb.

The instrument response functions (IRFs; P8R3\_SOURCE\_V3) is used. The main background component consists of charged particles that are misclassified as gamma-rays. It is included in the analysis using the isotropic emission template (“iso\_P8R3\_SOURCE\_V3.v1.txt”). As the GRB is located at the high Galactic latitude, the contribution from the Galactic diffuse emissions is very small, which is accounted for by using the diffuse Galactic interstellar emission template (IEM, gll\_iem\_v07.fits). The parameter of isotropic emission is left free and the one of IEM is fixed. We note that one 4FGL source (4FGL J1410.4+2820) is close to the GRB ( $0.55^\circ$  from Swift/XRT position). We estimate its  $\sim 13.3$  years average flux before the GRB trigger to be  $(1.59 \pm 0.41) \times 10^{-9}$  photons  $\text{cm}^{-2} \text{s}^{-1}$  (the light curve of 4FGL J1410.4+2820 is shown in Figure 1). This flux implies that this source is not bright enough to be considered as the background source in the model.

The data analysis was performed using the publicly available software fermitools (ver. 2.0.8) with the unbinned likelihood analysis method. Assuming a power-

law spectrum of the burst, we obtained the best-fit Fermi-LAT position of GRB 211211A in 395–30,780 s with the tool gtfndsrc: ( $212.60^\circ, 27.87^\circ$ ) with a circular error of  $0.20^\circ$  (statistical only). The maximum likelihood test statistic (TS) is used to estimate the significance of the GRB, which is defined by  $TS = 2(\ln \mathcal{L}_1 - \ln \mathcal{L}_0)$ , where  $\mathcal{L}_1$  and  $\mathcal{L}_0$  are maximum likelihood values for the background with the GRB and without the GRB (null hypothesis). Using the gttsmap tool, we evaluate the TS map in the vicinity of the GRB, which is shown in Figure 2. The maximum value,  $TS_{\max} = 50.82$ , is found at the location of R.A. =  $212.61^\circ$  and Decl. =  $27.91^\circ$  (J2000), consistent with the result of gtfndsrc. This  $TS_{\max}$  value corresponds to a detection significance of  $6.2\sigma$  or  $6.7\sigma$  (one-sided) if the  $TS_{\max}$  distribution follows  $(1/2)\chi_4^2$  or  $(1/2)\chi_2^2$ , respectively<sup>2</sup>. We compute the error contours of the source localization using the method suggested by Fermi-LAT Collaboration et al. (2021), and the isocontours containing localization probabilities of 68% and 90% are shown as green lines in Figure 2. We find that the GRB position detected by Swift is inside the region of the localization contours of LAT at the 90% confidence level.

As part of our analysis, we use the gtsrprob tool to estimate the probability that each photon detected by the LAT is associated with the GRB. The list of events associated with the GRB with a probability higher than 80% is shown in Table 1, among which six photons have the probability higher than 90%. The first  $\gamma$ -ray photon with the probability exceeding 90% arrives at  $T_0 + 6438.83$  s, with an energy of 206.91 MeV, and the highest-energy photon is a 1740.45 MeV photon arriving at  $T_0 + 12967.39$  s.

The averaged flux is  $(3.23 \pm 0.86) \times 10^{-10}$  erg  $\text{cm}^{-2} \text{s}^{-1}$  with a photon index  $\Gamma_{\text{LAT}} = -3.30 \pm 0.45$  in 395–30,780 s. Assuming that the GRB occurs at a distance of 350 Mpc, the measured value of the flux corresponds to a luminosity of  $(4.74 \pm 1.26) \times 10^{45}$  erg  $\text{s}^{-1}$ . Figure 3 shows the temporal behavior and the spectrum of the GeV emission from GRB 211211A.

## 3. INTERPRETATION OF THE GEV EMISSION

Extended high-energy ( $> 100$  MeV) gamma-ray emission that lasts much longer than the prompt sub-MeV emission has been detected from a large number of GRBs

<sup>2</sup> As interpreted in the first LAT GRB catalogue (Ackermann et al. 2013), the model for a GRB analysis usually has 4 degrees of freedom, i.e., the two coordinates (e.g. (R.A., Decl.)) of the GRB and two spectral parameters. However, when an external position is used in the analysis (for example, the Swift/XRT initial position here), only 2 degrees of freedom are left.

<sup>1</sup> <https://fermi.gsfc.nasa.gov>

by Fermi-LAT. Before Fermi, extended GeV emission has been detected from GRB 940217 by EGRET (Hurley et al. 1994), with one 18 GeV photon arriving at about 5000 s after the burst. A plausible scenario for the extended high-energy emission is that it is the afterglow synchrotron emission produced by electrons accelerated in the forward shocks (Kumar & Barniol Duran 2010; Ghirlanda et al. 2010; Wang et al. 2010). In particular, high-energy ( $> 100$  MeV) emission is detected up to  $\sim 100$  s in the short GRB 090510 (Abdo et al. 2009). The multiwavelength (0.1-10 GeV, X-ray, and optical) emission of GRB 090510 can be explained via synchrotron emission from an adiabatic forward shock propagating into a homogeneous ambient medium (He et al. 2011). However, since the maximum synchrotron photon energy for accelerated electrons under the most favorable condition (i.e., the Bohm acceleration) is about 50 MeV in the shock rest frame and the bulk Lorentz factor of the external shock decreases with time, it is a challenge to explain  $> 10$  GeV photons detected from GRB afterglows (Barniol Duran & Kumar 2011; Piran & Nakar 2010; Sagi & Nakar 2012). In fact, recent detection of sub-TeV emission from a few GRBs has been interpreted as arising from the inverse-Compton (IC) emission of the afterglow (MAGIC Collaboration et al. 2019; Derishev & Piran 2021; Wang et al. 2019).

The maximum energy of the photons detected from GRB 211211A is only 1.7 GeV, so it is reasonable to consider the afterglow synchrotron emission scenario. Below we study the possibility of the forward shock emitting the GeV afterglow emission. We perform modeling of the Fermi-LAT data for GRB 211211A using a numerical code developed in our previous work (Liu et al. 2013). According to the standard afterglow model (Sari et al. 1998), the light curve for a given observed frequency ( $\nu$ ) could be calculated as  $F(t, \nu) = F(t, \nu, E_{k, \text{iso}}, n, p, \varepsilon_e, \varepsilon_B, \Gamma_0, \theta_j)$ . Here  $E_{k, \text{iso}}$  is the isotropic kinetic energy of the GRB outflow,  $n$  is the particle number density of the ambient medium,  $p$  is the electron spectral index,  $\varepsilon_e$  and  $\varepsilon_B$  are the equipartition factors for the energy in electrons and magnetic field in the shock,  $\Gamma_0$  is the initial Lorentz factor of the outflow, and  $\theta_j$  is the half-opening angle of the jet. In this code, the electrons that produce synchrotron high-energy emission also undergo IC loss and the Klein-Nishina (KN) effect has been taken into account (Wang et al. 2010). We find that the model can reproduce the light curves of GeV and X-ray afterglows, as well as the optical afterglow at early time when the kilonova emission is subdominant (Rastinejad et al. 2022), for the following parameter values:  $E_{k, \text{iso}} = 1 \times 10^{53}$  erg,  $\Gamma_0 = 100$ ,  $n = 10^{-4}$  cm $^{-3}$ ,  $p = 2.2$ ,

$\varepsilon_e = 0.1$ ,  $\varepsilon_B = 6 \times 10^{-5}$  and  $\theta_j = 1.0^\circ$  (see Figure 3). The measured photon index of the X-ray afterglow by Swift/XRT ( $\Gamma_X = -1.5_{-0.06}^{+1.2}$ ; Osborne et al. (2021)) is also consistent with  $p = 2.2$ , as the X-ray frequency locates in the regime  $\nu_m < \nu_X < \nu_c$ , where  $\nu_m$  and  $\nu_c$  are, respectively, the frequencies corresponding to the injection break and cooling break (Sari et al. 1998). We note that the observed X-ray flux at 3-5 ks exceeds the model flux to some extent, which could indicate that the early X-ray emission may have some contribution from an extra component other than the afterglow, such as the central engine activity, as have been seen in some GRB X-ray afterglows (Troja et al. 2007).

To explain the long-duration of the GeV emission, a long deceleration time for the external shock is needed. This implies a low density of  $n \simeq 10^{-4}$  cm $^{-3}$ . Such a low density of the ambient medium is not surprising, since the GRB lies outside of the optical disk of the host galaxy, consistent with the compact stellar merger scenario. In addition, Quasi-Periodic Oscillations (QPO) with frequency  $\simeq 22$  Hz are found throughout the precursor of GRB 211211A (Xiao et al. 2022), which indicates most likely that a magnetar participated in the merger. The pulsar wind from the magnetar may have created a cavity around the pulsar (Holcomb et al. 2014).

The spectrum measured by Fermi-LAT appears softer than the predicted synchrotron spectrum  $F_{\text{GeV}} \sim \nu^{-p/2}$ . One solution to this problem is assuming a maximum cutoff energy for the synchrotron emission, which is related to the maximum energy of shock-accelerated electrons. By equating the synchrotron cooling time with the acceleration time, we get the maximum Lorentz factor of the accelerated electrons,  $\gamma_M = \sqrt{(6\pi e \eta_{\text{acc}})/(\sigma_T(1+Y)B)}$ , where  $\eta_{\text{acc}}$  is the acceleration efficiency,  $\sigma_T$  is the Thompson scattering cross section,  $Y$  is the Compton parameter for IC emission and  $B$  is the magnetic field. We find that assuming  $\eta_{\text{acc}} = 0.01$ , the GeV spectrum of GRB 211211A can be reproduced by the model. This implies that the Bohm acceleration approximation breaks down at such high energies, possibly due to the small-scale nature of the microturbulent magnetic field behind the shock (Wang et al. 2013).

#### 4. SUMMARY

We reported the detection of a GeV afterglow from GRB 211211A, which is a long-duration GRB, but results from a compact stellar merger. The GeV emission continues up to about 20,000 s after the burst. The duration is the longest one compared to the GeV afterglows of other short-duration GRBs (see the Extended Data Fig. 7 in Fermi-LAT Collaboration et al. (2021)).

However, it is quite similar to the long-duration GRB 940217 (Hurley et al. 1994), which has one 18 GeV photon at about 5000 s after the burst. It has been suggested that the late GeV emission of GRB 940217 may be produced by the synchrotron-self Compton (SSC) emission of the afterglow (Dermer et al. 2000; Zhang & Mészáros 2001). However, for GRB 211211A, it is hard to reproduce the GeV peak at 20,000 s with SSC emission given the constraint from the X-ray and optical afterglows. In addition, since GRB 211211A occurs at the position outside the galaxy disk, the density of the circumburst medium is expected to be low, which leads to a subdominant contribution to the GeV emission by the SSC component. Instead, we find that the GeV emission of GRB 211211A can be interpreted as arising from the afterglow synchrotron emission. The soft spectrum of the GeV emission could arise from a limited maximum

synchrotron energy of only a few hundreds of MeV at  $\sim 20,000$  s. The long duration of the GeV emission can be interpreted as the long deceleration time due to a low-density circumburst environment, which agrees well with the density environment expected for compact stellar mergers.

#### ACKNOWLEDGMENTS

The work is supported by the NSFC Grants No.12121003 and No. U2031105, the National Key R&D program of China under Grant No. 2018YFA0404203, and China Manned Space Project (CMS-CSST-2021-B11).

While we were preparing the final submission, we became aware of the work by Mei et al. (2022), which also reports the detection of GeV emission from GRB 211211A. The two works are independent of each other.

#### REFERENCES

- Abbott, B. P., Abbott, R., Abbott, T. D., et al. 2017, *ApJL*, 848, L12, doi: [10.3847/2041-8213/aa91c9](https://doi.org/10.3847/2041-8213/aa91c9)
- Abdo, A. A., Ackermann, M., Ajello, M., et al. 2009, *ApJL*, 706, L138, doi: [10.1088/0004-637X/706/1/L138](https://doi.org/10.1088/0004-637X/706/1/L138)
- Abdollahi, S., Acero, F., Ackermann, M., et al. 2020, *ApJS*, 247, 33, doi: [10.3847/1538-4365/ab6bcb](https://doi.org/10.3847/1538-4365/ab6bcb)
- Ackermann, M., Ajello, M., Asano, K., et al. 2013, *ApJS*, 209, 11, doi: [10.1088/0067-0049/209/1/11](https://doi.org/10.1088/0067-0049/209/1/11)
- Ahumada, T., Singer, L. P., Anand, S., et al. 2021, *Nature Astronomy*, 5, 917, doi: [10.1038/s41550-021-01428-7](https://doi.org/10.1038/s41550-021-01428-7)
- Ajello, M., Allafort, A., Axelsson, M., et al. 2018, *ApJ*, 861, 85, doi: [10.3847/1538-4357/aac515](https://doi.org/10.3847/1538-4357/aac515)
- Barniol Duran, R., & Kumar, P. 2011, *MNRAS*, 412, 522, doi: [10.1111/j.1365-2966.2010.17927.x](https://doi.org/10.1111/j.1365-2966.2010.17927.x)
- Barthelmy, S. D., Barbier, L. M., Cummings, J. R., et al. 2005, *SSRv*, 120, 143, doi: [10.1007/s11214-005-5096-3](https://doi.org/10.1007/s11214-005-5096-3)
- D’Ai, A., Ambrosi, E., D’Elia, V., et al. 2021, *GRB Coordinates Network*, 31202, 1
- Derishev, E., & Piran, T. 2021, *ApJ*, 923, 135, doi: [10.3847/1538-4357/ac2dec](https://doi.org/10.3847/1538-4357/ac2dec)
- Dermer, C. D., Chiang, J., & Mitman, K. E. 2000, *ApJ*, 537, 785, doi: [10.1086/309061](https://doi.org/10.1086/309061)
- Evans, P. A., Beardmore, A. P., Page, K. L., et al. 2007, *A&A*, 469, 379, doi: [10.1051/0004-6361:20077530](https://doi.org/10.1051/0004-6361:20077530)
- . 2009, *MNRAS*, 397, 1177, doi: [10.1111/j.1365-2966.2009.14913.x](https://doi.org/10.1111/j.1365-2966.2009.14913.x)
- Fermi-LAT Collaboration, Ajello, M., Atwood, W. B., et al. 2021, *Nature Astronomy*, 5, 385, doi: [10.1038/s41550-020-01287-8](https://doi.org/10.1038/s41550-020-01287-8)
- Gal-Yam, A., Fox, D. B., Price, P. A., et al. 2006, *Nature*, 444, 1053, doi: [10.1038/nature05373](https://doi.org/10.1038/nature05373)
- Galama, T. J., Vreeswijk, P. M., van Paradijs, J., et al. 1998, *Nature*, 395, 670, doi: [10.1038/27150](https://doi.org/10.1038/27150)
- Gehrels, N., Norris, J. P., Barthelmy, S. D., et al. 2006, *Nature*, 444, 1044, doi: [10.1038/nature05376](https://doi.org/10.1038/nature05376)
- Ghirlanda, G., Ghisellini, G., & Nava, L. 2010, *A&A*, 510, L7, doi: [10.1051/0004-6361/200913980](https://doi.org/10.1051/0004-6361/200913980)
- Gompertz, B. P., Rivasio, M. E., Nicholl, M., et al. 2022, *arXiv e-prints*, arXiv:2205.05008, <https://arxiv.org/abs/2205.05008>
- He, H.-N., Wu, X.-F., Toma, K., Wang, X.-Y., & Mészáros, P. 2011, *ApJ*, 733, 22, doi: [10.1088/0004-637X/733/1/22](https://doi.org/10.1088/0004-637X/733/1/22)
- Holcomb, C., Ramirez-Ruiz, E., De Colle, F., & Montes, G. 2014, *ApJL*, 790, L3, doi: [10.1088/2041-8205/790/1/L3](https://doi.org/10.1088/2041-8205/790/1/L3)
- Hurley, K., Dingus, B. L., Mukherjee, R., et al. 1994, *Nature*, 372, 652, doi: [10.1038/372652a0](https://doi.org/10.1038/372652a0)
- Kouveliotou, C., Meegan, C. A., Fishman, G. J., et al. 1993, *ApJL*, 413, L101, doi: [10.1086/186969](https://doi.org/10.1086/186969)
- Kumar, P., & Barniol Duran, R. 2010, *MNRAS*, 409, 226, doi: [10.1111/j.1365-2966.2010.17274.x](https://doi.org/10.1111/j.1365-2966.2010.17274.x)
- Liu, R.-Y., Wang, X.-Y., & Wu, X.-F. 2013, *ApJL*, 773, L20, doi: [10.1088/2041-8205/773/2/L20](https://doi.org/10.1088/2041-8205/773/2/L20)
- MAGIC Collaboration, Acciari, V. A., Ansoldi, S., et al. 2019, *Nature*, 575, 455, doi: [10.1038/s41586-019-1750-x](https://doi.org/10.1038/s41586-019-1750-x)
- Mangan, J., Dunwoody, R., Meegan, C., & Fermi GBM Team. 2021, *GRB Coordinates Network*, 31210, 1
- Meegan, C., Lichti, G., Bhat, P. N., et al. 2009, *ApJ*, 702, 791, doi: [10.1088/0004-637X/702/1/791](https://doi.org/10.1088/0004-637X/702/1/791)

- Mei, A., Banerjee, B., Oganessian, G., et al. 2022, arXiv e-prints, arXiv:2205.08566.  
<https://arxiv.org/abs/2205.08566>
- Norris, J. P., Cline, T. L., Desai, U. D., & Teegarden, B. J. 1984, *Nature*, 308, 434, doi: [10.1038/308434a0](https://doi.org/10.1038/308434a0)
- Osborne, J. P., Page, K. L., Ambrosi, E., et al. 2021, GRB Coordinates Network, 31212, 1
- Piran, T., & Nakar, E. 2010, *ApJL*, 718, L63, doi: [10.1088/2041-8205/718/2/L63](https://doi.org/10.1088/2041-8205/718/2/L63)
- Rastinejad, J. C., Gompertz, B. P., Levan, A. J., et al. 2022, arXiv e-prints, arXiv:2204.10864.  
<https://arxiv.org/abs/2204.10864>
- Sagi, E., & Nakar, E. 2012, *ApJ*, 749, 80, doi: [10.1088/0004-637X/749/1/80](https://doi.org/10.1088/0004-637X/749/1/80)
- Sari, R., Piran, T., & Narayan, R. 1998, *ApJL*, 497, L17, doi: [10.1086/311269](https://doi.org/10.1086/311269)
- Troja, E., Cusumano, G., O'Brien, P. T., et al. 2007, *ApJ*, 665, 599, doi: [10.1086/519450](https://doi.org/10.1086/519450)
- Wang, X.-Y., He, H.-N., Li, Z., Wu, X.-F., & Dai, Z.-G. 2010, *ApJ*, 712, 1232, doi: [10.1088/0004-637X/712/2/1232](https://doi.org/10.1088/0004-637X/712/2/1232)
- Wang, X.-Y., Liu, R.-Y., & Lemoine, M. 2013, *ApJL*, 771, L33, doi: [10.1088/2041-8205/771/2/L33](https://doi.org/10.1088/2041-8205/771/2/L33)
- Wang, X.-Y., Liu, R.-Y., Zhang, H.-M., Xi, S.-Q., & Zhang, B. 2019, *ApJ*, 884, 117, doi: [10.3847/1538-4357/ab426c](https://doi.org/10.3847/1538-4357/ab426c)
- Xiao, S., Zhang, Y.-Q., Zhu, Z.-P., et al. 2022, arXiv e-prints, arXiv:2205.02186.  
<https://arxiv.org/abs/2205.02186>
- Yang, J., Zhang, B. B., Ai, S. K., et al. 2022, arXiv e-prints, arXiv:2204.12771. <https://arxiv.org/abs/2204.12771>
- Zhang, B., & Mészáros, P. 2001, *ApJ*, 559, 110, doi: [10.1086/322400](https://doi.org/10.1086/322400)
- Zhang, B. B., Liu, Z. K., Peng, Z. K., et al. 2021, *Nature Astronomy*, 5, 911, doi: [10.1038/s41550-021-01395-z](https://doi.org/10.1038/s41550-021-01395-z)

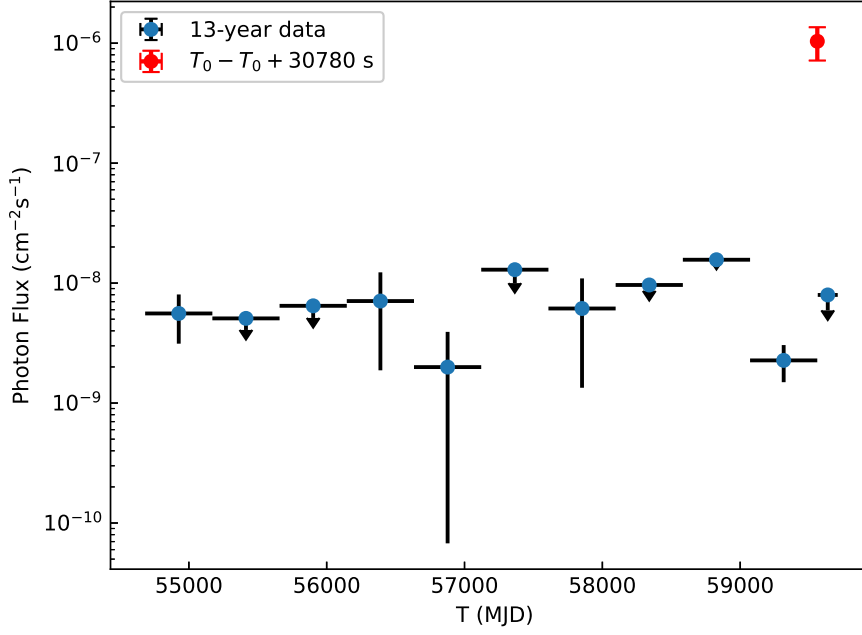


**Figure 1.** Light curve of 4FGL J1410.4+2820 in 0.1-10 GeV (blue data) in comparison with the GeV flux (red data) from GRB 211211A.

**Table 1.** List of the selected gamma-ray events with a probability of association  $> 80\%$  in 395-30780 s.

Time since $T_0$ (s)	Energy(MeV)	R.A.(deg)	Decl.(deg)	Probability(%)
1165.89	400.05	213.28	27.25	86.80
6238.33	142.38	212.64	29.01	84.18
6438.83	206.91	212.67	27.82	90.42
6648.08	187.58	212.11	28.91	90.91
12494.06	163.96	212.57	29.20	89.95
12967.39	1740.45	212.63	27.85	98.91
13054.08	102.64	211.48	28.20	94.41
17410.06	113.83	211.61	27.22	92.45
17861.10	286.10	213.34	28.65	88.36
18128.17	231.49	212.80	28.36	94.83
24487.04	104.01	214.33	29.19	88.31
28335.50	274.59	212.37	26.89	88.35

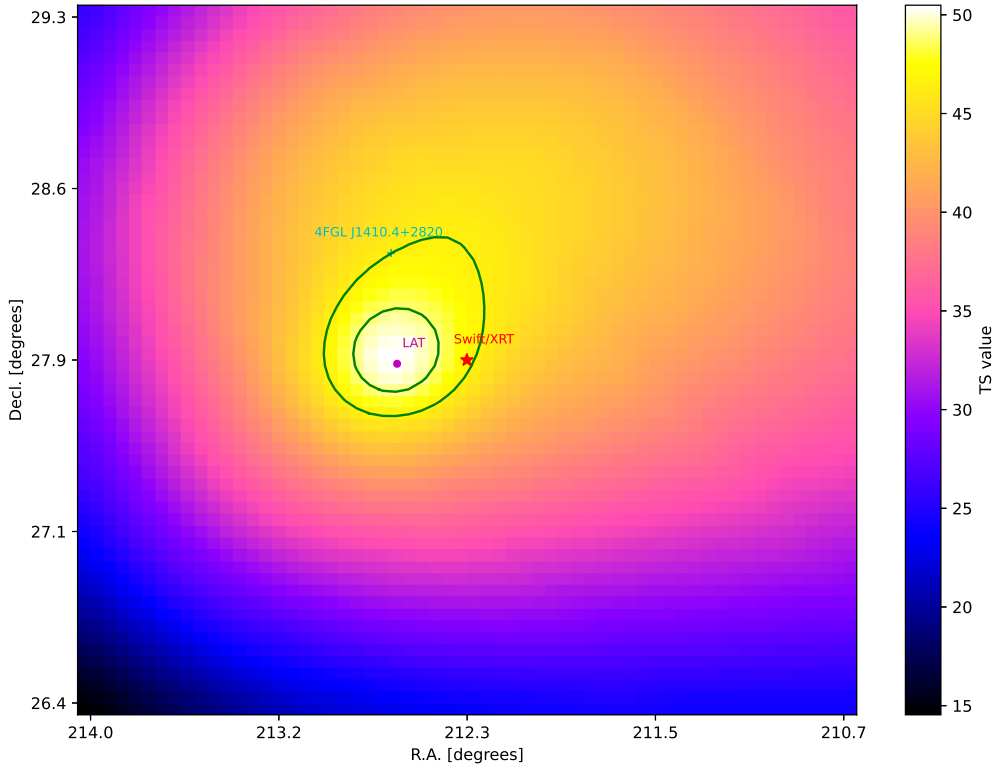


**Figure 2.**  $3^\circ \times 3^\circ$  TS map of the gamma-ray emission in 0.1–10 GeV measured by Fermi-LAT around GRB 211211A in 395–30780 s after the BAT trigger. The cyan cross represents 4FGL J1410.4+2820, which is suggested to be associated with a BL Lacertae RX J1410.4+2821 by Fermi-LAT Collaboration (Abdollahi et al. 2020). The magenta point indicates the best localization of GRB 211211A. The two green lines represent the localization contours of GRB 211211A at 68% and 90% confidence levels, respectively. The red star represents the localization of GRB 211211A by Swift/XRT (D’Ai et al. 2021).

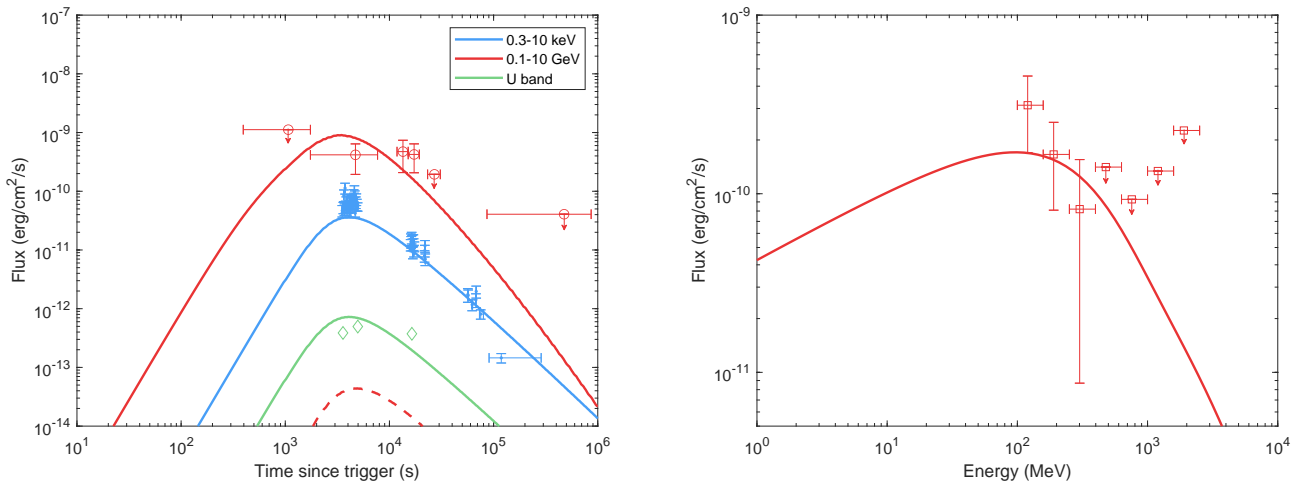


**Figure 3.** Left panel: light curves of the GeV emission of GRB 211211A measured by Fermi-LAT and the modeling of the multi-wavelength afterglow light curves. The red, blue and green data points represent the GeV, X-ray and early optical flux of GRB 211211A, respectively. X-ray data are downloaded from the UK Swift Science Data Centre (UKSSDC; Evans et al. (2007, 2009)). The optical data are obtained from Rastinejad et al. (2022). The solid lines represent the synchrotron emission at GeV, X-ray and optical bands, while the dashed line represents the SSC component at the GeV band in our modeling. Right panel: the measured spectrum and modeling of the GeV emission of GRB 211211A during 395–30780 s. The parameters used in the modeling are  $E_{k,iso} = 1 \times 10^{53}$  erg,  $\Gamma_0 = 100$ ,  $n = 10^{-4}$  cm $^{-3}$ ,  $p = 2.2$ ,  $\varepsilon_e = 0.1$ ,  $\varepsilon_B = 6 \times 10^{-5}$ ,  $\theta_j = 1.0^\circ$  and  $\eta_{acc} = 0.01$  (see the text for more details).